On Water Flowing Out From Two Parallel Holes

Johnathan Bressler and Offek Tziperman, Advised By: Shmuel Rubinstein

Abstract

The dynamics of water jets have been studied for centuries but the simple case of two parallel jets has not received much attention. We study the two phases of outflowing water from two parallel holes, a single combined jet and separate twin jets. We find that the distinction between the phases can be well described as a competition between surface tension and inertia. The phase transition was found to occur at a critical hydrostatic pressure. The effects of friction were calculated and measured to find the exit velocity of the jets. We model the transition using a key parameter S, where $S = 1$ marks the split. Our model takes into account the radii of the holes, the distance between them, the surface tension and the outflow velocity of the jets. The parameter space was scanned experimentally for Reynolds numbers ranging between 5 and 900, and the experimental data agreed well with the model.

1 Introduction

Jets of water have been studied for centuries. In 1878 Lord Rayleigh showed the disintegration of jets of water into drops can be explained by external perturbations growing due to the effects surface tension [1]. Collisions of water jets can form exotic structures. [2] Studied the collisions of jets at an angle and the structures formed post collision. Head on collisions of jets have also been investigated [3], but the simple case of two parallel jets, as in the case of water flowing from two holes, has not yet received much attention.

Consider a tall tank of water with two small circular holes at the bottom. The two jets leaving the tank may combine to form one or flow out separately. Single and twin jet phases can both be seen, for a given set of holes, by changing the hydrostatic pressure at the bottom of the tank. At low pressure, the jets flow out at low velocity and the forces of surface tension combine them into one. At high pressures the outflow velocity is high and the jets do not combine.

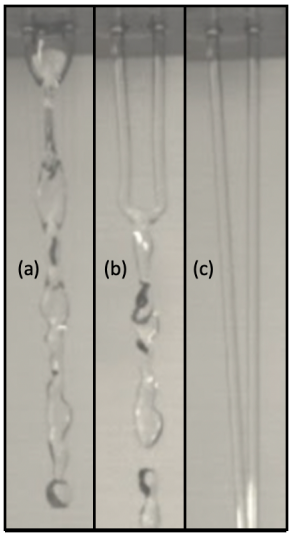

Figure 1.1: The Phases of Jet Flow
Photos taken with a high speed camera of the two phases and the transition between them. (a) The combined jet phase. The two jets combine into one to form a liquid surface. Bellow, a chain like shape of water flow can be seen. (b) The transition between phases. The liquid surface is torn from the top splitting into two. The connection between the jets moves downwards until eventually the stream is in a two jet phase. (c) The two jet phase. Water flows from the tank in two separate streams.

When the jets are combined they form a sheet of

water. Below the sheet, the water flows in a chain like shape. At a certain point the chain breaks up into drops due to Rayleigh instability (Fig 1.1a). [2] found the chain like flow to be a result of the joined effects of surface tension and inertia. As the pressure is increased the sheet thins until eventually rupturing from the surface and breaking into two jets. If the pressure is then lowered back, the jets stay split through a large drop in pressure, showing hysteresis. In this work we experimentally study the phase transitions between the combined and twin jet states. We examine the critical hydrostatic pressure for the split of the jets varying the different parameters. R, radii of holes. D, the distance between holes. γ the surface tension and μ the dynamic viscosity.

In §2 we study the dependance of the critical pressure (P_c) for the phase transition as a function of R and D. In §3 we use glycerol and water solutions to study the dependance of P_c on the viscosity of the fluid. In §4 we use water soap solutions to measure the dependance on the surface tension. In §5 we model the losses to friction using the Darcy Weisbach equation and compare to experiments. In §6 we introduce a parameter S that determines the phase transition. In §7 we conclude.

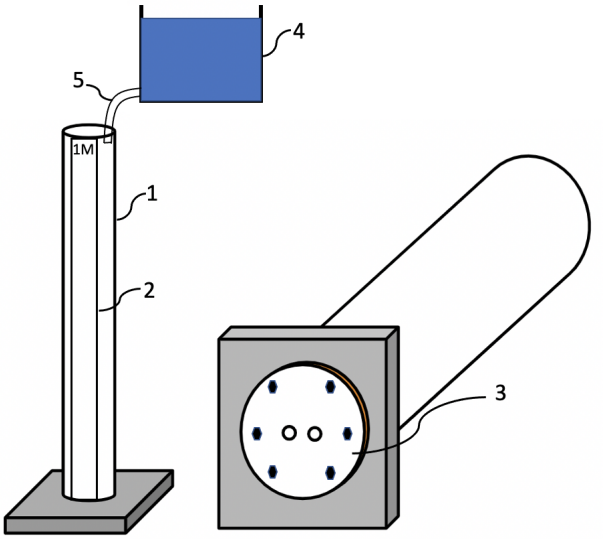

Figure 2.1: Experimental Setup - Critical Pressure. Experimental setup for the measurement of the critical hydrostatic pressure for the phase transition. (1) A 1 meter length PMMA pipe. (2) A tape measure glued on the outside of the tank allowing measurement of the water height. (3) A screw-on cap with two circular holes. The sample consisted of 39 caps with changing radii and distance between the holes. (4) A tank of water used to poor water into the PMMA pipe using a smaller tube (5), which allows control of the hydrostatic pressure at the bottom. A sponge was connected to the end of the tube, reducing the perturbations due to the water inflow from the upper tank.

2 Critical Pressure as Function of Radii and Distance

To measure the critical hydrostatic pressure we used as our tank a one meter length PMMA pipe. The pipe was open on one side and closed with a changeable cap on the other. This allowed changing the holes at the bottom of the tank by changing caps. The pipe diameter was 40 mm. The caps were 2 mm thick PMMA disks with two circular holes near the center (Fig 2) which had modulated radii and distance between them.

Each measurement initiates when liquid coming out of two holes merges into a single stream. Liquid flows from a higher tank into the pipe and fills it up increasing the pressure at the bottom. When the pressure is at its critical value and the jet splits into two, the height of the liquid in the tank (h_c) was measured using a tape measure fixed to the pipe. Each measurement was taken three times, and the three consecutive measurements were then averaged. All measurements were taken at room temperature. Then the critical hydrostatic pressure was calculated using:

$$P_c = \rho g h_c, \tag{2.1}$$

where ρ is the density of the measured liquid and $g = 9.81\left[\frac{m}{s}\right]$.

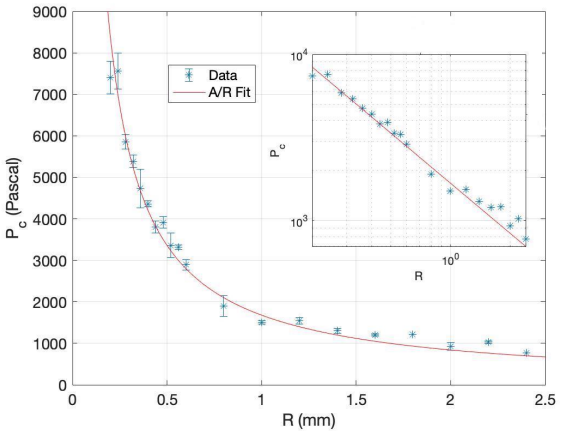

Figure 2.2: P_c vs. Holes Radii
Measurement of P_c as a function of R the hole radius with a $y = A/R$ fit. The inset is the same plot in logarithmic scale. The fit parameter is $A = 1679$ (Pascal·mm). $D = 2\ [mm]$, $\mu = 0.00089\ [Pa \cdot s]$, $\gamma = 0.0375\ [N/m]$ are kept constant.

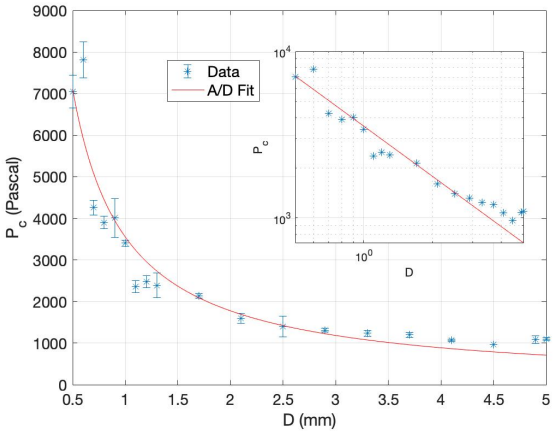

Figure 2.3: P_c vs. Distance Between Holes
Measurement of the critical hydrostatic pressure for the split as a function of the distance between holes perimeter with a $y = A/D$ fit. The inset is the same plot in logarithmic scale. The fit parameter is $A = 3550$ (Pascal·mm). $R = 0.5\ [mm]$, $\mu = 0.00089\ [Pa \cdot s]$,$\gamma = 0.0375\ [N/m]$ are kept constant.

P_c shows a dependance of R^{-1} with the other parameters kept constant (Fig 2.2). This is due mostly to the friction losses in the holes. The losses have a strong dependance on radii. In cases of larger radii, there are less losses to friction. Hence, the velocities of the jets exiting the tank are larger. This increases the inertia compared to the surface tension, lowering the critical pressure for the split. This dependance on R will probably break down when $R \to 0$, but holds for the regime measured in our experiments. We further look into the effects of friction in §5.

P_c also shows a dependance of D^{-1}, as shown in (Fig 2.3). When D is large, the jets have a long way to go before they can combine. Increasing D increases the inertia compared to the surface tension. P_c diverges as $D \to 0$ as the two holes become one.

3 Critical Pressure as Function of Viscosity at $Re < 1$

The dependance of critical height on viscosity (μ) was measured using different solutions of glycerol and water in the PMMA pipe. Viscosity and surface tension of each concentration of glycerol and water were obtained from [4], and the critical hight was measured as described in §2. The density and surface tension of the solutions differ only slightly and were considered negligible.

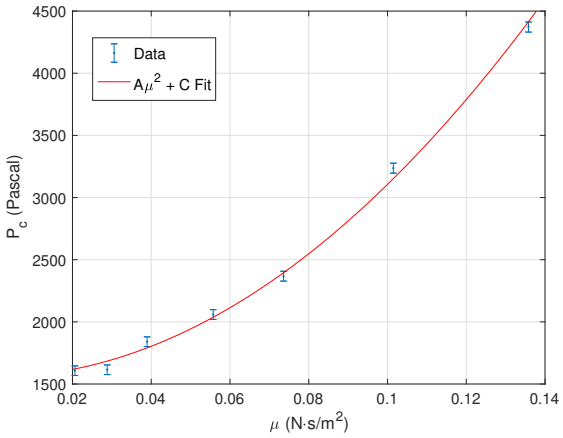

Figure 3.1: Critical Hydrostatic Pressure as a Function of Dynamic Viscosity
Measurement of the critical hydrostatic pressure for the split as a function of μ the dynamic viscosity. The fit parameters are $A = 1.55{\cdot}10^5$ (m/kg), $C = 1556$ (Pascal). $R = 0.7\ [mm], D = 2\ [mm], \gamma = 0.0375\ [N/m]$ are kept constant. Viscosity was changed using glycerol and water solutions. The data shown is in the laminar regime with Reynolds number $0.06 < Re < 1.07$. In this regime $P_c \propto \mu^2$.

Increasing μ increases the friction losses in the holes. Thus a higher concentration of glycerol corresponds to a lower exit velocity, weakening the inertia compared to surface tension, and increasing P_c.

4 Surface Tension

In this section, P_c was measured as a function of surface tension. Surface tension of different solutions of soap and water, was measured in Jaeger's method [5]. Soap reduces the solution's surface tension. A 2 mm diameter pipe was connected on one side to a syringe filled with air. The other side was connected into a glass pipet with a narrow tip of 1 mm radius ($2R$). The pipet tip was fixed 4 cm (h) underwater in a cup , and leveled perpendicular to the water surface with a spirit level (Fig. 4.1). A T-shaped pipe joint connected the pipe into the pressure gauge. The pressure gauge was an open ended curved pipe containing water with food coloring.

Water and soap solutions were poured into the cup. By compressing air steadily with the syringe, an air bubble inflated out the tip in an approximately spherical shape. The colored water was pushed accordingly. The curved pipe was filmed and the displacement hight (H) measured in pixels.

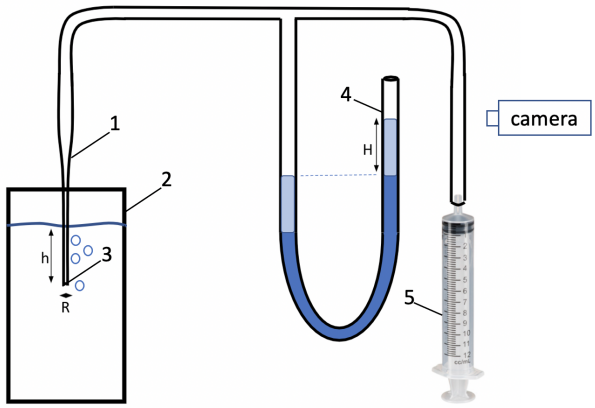

Figure 4.1: Experimental Setup - Surface Tension.
The Jaeger setup for measuring surface tension. (1) A pipet is inserted 4 cm inside a cup of the measured liquid (2). (3) At the edge of the pipet an air bubble fills up with increasing curvature. Once half the air bubble is outside the pipet it becomes unstable and escapes. At this moment, the height of the water in the pressure gauge (4) is measured. The air bubble is filled with air using a syringe (5). The height H was measured by filming with a high speed camera and using a tape measure to convert from pixels to cm.

The Young–Laplace equation [6] connects the pressure difference with the geometric curvature:

$$\Delta p = \gamma \left(\frac{1}{R_1} + \frac{1}{R_2} \right), \tag{4.1}$$

where γ stands for the surface tension of the liquid and R_1, R_2 are the radii of curvature. The shape of the drop was approximately spherical such that $R_1 \sim R_2 \sim R$. When the drop shape is a half sphere outside the pipet, the drop becomes unstable and exits. The pressure drop was calculated by equating

the hydrostatic pressure difference across the bubble and the pressure difference across the curved pipe:

$$\Delta p = 2\rho g H - \rho g h. \tag{4.2}$$

Using (4.1) we have:

$$\gamma = \rho g R \left(H - \frac{h}{2} \right). \tag{4.3}$$

For each water and soap solution, surface tension was measured three times and the results were averaged. After each measurement of surface tension, the same solution was used to measure the critical hight as described in §2.1.

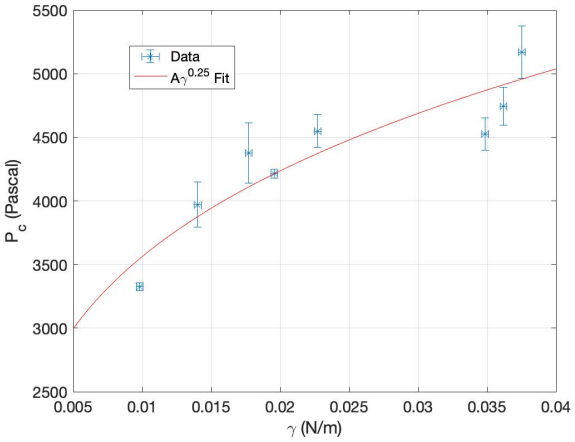

Figure 4.2: P_c vs Surface Tension
Measurement of the critical hydrostatic pressure for the split as a function of γ the surface tension. The fit parameter is $A = 1.126 \cdot 10^4 \ \left(\mathrm{N}^{0.75} \cdot \mathrm{m}^{-1.75}\right)$. The surface tension of the water soap mixtures was measured using the Jaeger setup. $R = 0.18 \ [mm], D = 2 \ [mm], \mu = 0.00089 \ [Pa \cdot s]$ are kept constant. Surface tension was changed by adding soap and measured using the Jaegerś method. In the regime measured $P_c \propto \gamma^{1/4}$ roughly.

P_c has a very weak dependance on surface tension. Nevertheless, a significant effect can be seen. Raising the surface tension increases P_c as the inertia does not change much.

5 Losses to Friction in the Holes

5.1 Theoretical Model for Friction

We model the friction losses in the holes as losses in pipes using the Darcy Weisbach (DW) equation [7]. For laminar flow in a pipe the equation takes the form:

$$\Delta P_{loss} = \beta \frac{\mu v}{R^2} L, \tag{5.1}$$

where ρ is the density, v is flow velocity, L is the length of the pipe, R is the radius and β is a dimensionless free parameter. Using the Bernoulli equation:

$$\frac{1}{2}\rho v_1^2 + P_1 + \rho g h_1 - \Delta P_{loss} = \frac{1}{2}\rho v_2^2 + P_2 + \rho g h_2, \tag{5.2}$$

where the indices 1 and 2 correspond to the top and bottom of the water in the tank respectively. Since the pressure at the top and bottom of the tank are atmospheric we have $P_1 = P_2 = P_{atm}$. The cross-section area of the tank is much larger than the area of the holes and thus $v_1 \approx 0$. By definition, $h_2 = 0$, (5.2) simplifies to:

$$v_2^2 + 2\frac{\beta \mu L}{\rho R^2} v_2 - 2 g h_1 = 0. \tag{5.3}$$

The equation is a second degree polynomial. Neglecting the non physical negative solution, and replacing $v_2 = V_{out}, \ h_2 = h$ we arrive at:

$$V_{out} = -\frac{\beta \mu}{\rho R^2} L + \sqrt{\frac{\beta^2 \mu^2 L^2}{\rho^2 R^4} + 2gh}. \tag{5.4}$$

5.2 Comparison of Friction Model to Experiments

To measure the outward velocity of the jets considering the losses to friction, we filmed the tank of water with a high speed camera. A small floating cube was placed in the tank and tracked. The image analysis was done using Tracker computer program. In this way we obtain the height of water in the tank ($h_T(t)$). Invoking conservation of volume, approximating the water as incompressible:

$$V_{out} A_H = \frac{dh_T}{dt} A_T. \tag{5.5}$$

where A_H and A_T are the cross-section area of the holes and tank respectively. Using the relations

$$A_T = \pi R_T^2, \tag{5.6}$$

$$A_H = 2\pi R_H^2, \tag{5.7}$$

we obtain:

$$V_{out} = \frac{dh_T}{dt}\frac{R_T^2}{2R_H^2}. \tag{5.8}$$

The measurements of V_{out} as a function of R are presented in (Fig 5.1). The data agrees with the model for low radii corresponding to low Reynolds numbers, at high radii a slight deviation can be seen due to entering the turbulent regime. In this regime, the DW equation does not hold in this form. We extrapolate this data for low radii (the laminar regime where DW holds) assuming the friction is independent of D, γ to find the dependance of V_{out} on the different parameters in §6.

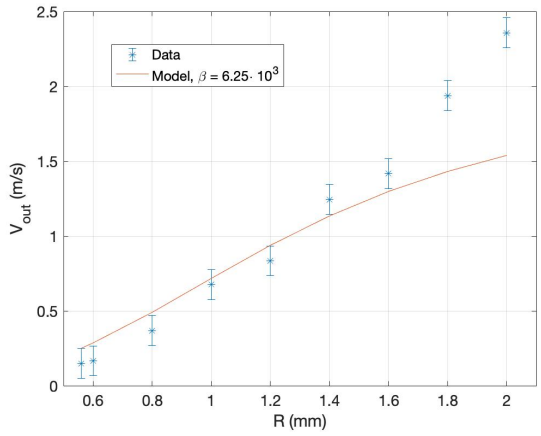

Figure 5.1: V_{out} as a function of R the hole radius
Measured jet outward velocity as a function of hole radius. The fit is given in equation (5.4) using $\beta = 6.25 \cdot 10^3$. The liquid used was pure water such that $\gamma = 0.0375\ [N/m]\,, d = 2\ [mm]$ and $\mu = 0.00089\ [Pa \cdot s]$ were kept constant. $\frac{dh_T}{dt}$ was measured at $h = 23\,[cm]$ for all radii.

6 Flow Streams in the Combined Jet Phase

In the single jet phase a sheet of water is formed underneath the two holes. In order to further understand the mechanism tearing the sheet of water it will be helpful to see the streamlines. In order to measure this, food coloring was injected into the tank while in a single jet state. The stream was filmed by a high speed camera and edited to increase contrast.

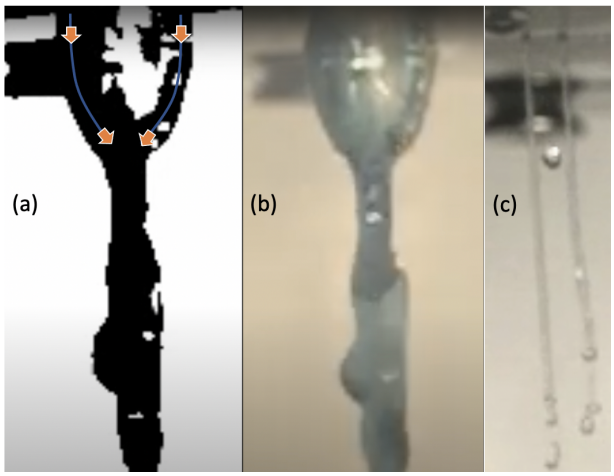

Figure 6.1: Stream Lines in the Sheet
Footage of the single jet phase with injected food coloring. Edited with interpreted stream lines (a) and unedited (b) . The liquid flows around the central drop and into the bottom jet. (c) The transition phase, as the liquid sheet tears and the connection of the jets falls, a drop of water can be seen bouncing between the jets.

The footage of the jet streamlines (Fig 6.1) shows flow near the outer edge of the liquid sheet. A drop is bounded between the two jets. The streamlines flow mostly around this drop with circulation of the water inside on a longer timescale, as can be seen in supplementary video 1.

Upon tearing of the liquid sheet the drop is sometimes left behind and can be seen bouncing on the jets during itś free-fall down. This can be seen in Fig 6.1c. On their way down, the jets pull on the drop. As the exit velocity increases the jets pull harder and harder

on the drop downwards. At the critical exit velocity the surface tension forces are not enough to accelerate the jets towards each other horizontally and the liquid sheet is broken.

7 A Parameter to Determine the Phase Transition

Using Buckingham π theorem[8], dimensional analysis strengthens the analytical model. Following 7, the relevant independent physical variables on which the model is based, are R, D, γ, g, ρ. Thus, three fundamental dimensions describes our system: meter, second and kg. Gathering the data, three dimensionless factors contains the experimental information:

$$\Pi_1 = \frac{R}{D}; \qquad \Pi_2 = \frac{\rho v^2 D}{\gamma}; \qquad \Pi_3 = \frac{Dg}{v^2}; \tag{7.1}$$

While Π_2 is the Weber No. that is used to compare the relative significance of fluid's surface tension compared to its inertia[9]. The three dimensional

$$\Pi_1 = 0.23 \cdot \Pi_2^{0.25} \Pi_3^{-0.25} \tag{7.2}$$

This relation attains a linear correlation between the factors. The transition between two phases is represented in the fitting line. In the case that $\Pi_1 > 0.23 \cdot \Pi_2^{0.25} \Pi_3^{-0.25}$ so, $v > \frac{R}{D} \sqrt[4]{\frac{g\gamma}{\rho}}$. Velocity that reaches the critical value causes the split.

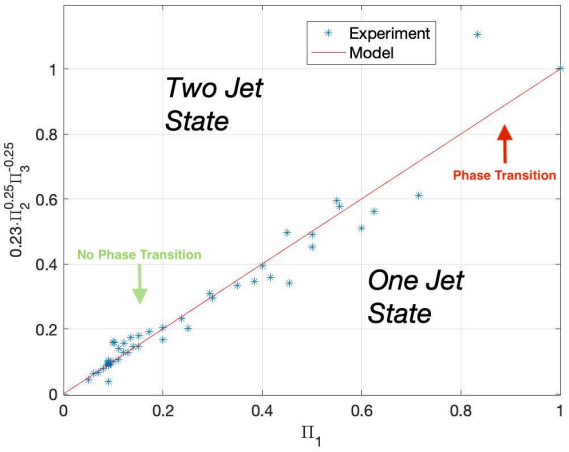

Figure 7.1: Π Factors
Measurements of differing γ, R, D presented in a single figure. $\Pi_1 = \frac{R}{D}; \Pi_2 = \frac{\rho V_{out}^2 D}{\gamma}; \Pi_3 = \frac{Dg}{V_{out}^2}$. Below the red line, $\Pi_1 > 0.23 \cdot \Pi_2^{0.25} \Pi_3^{-0.25}$, the system is in a single combined jet state. When raising the pressure and thus the outflow velocity, the system eventually reaches $S = 1$. This marks the transition into the two jet phase. Lowering the pressure back down, no phase transition is seen.

We can now define a critical parameter that determines the phase transition:

$$S = \frac{V_{out} D}{0.23R} \sqrt[4]{\frac{\rho}{g\gamma}}. \tag{7.3}$$

When coming from the low V_{out} regime reaching $S > S_c = 1$ marks the split. Returning back to $S < S_c$ the jets do not combine showing hysteresis.

8 Conclusions

We have experimentally investigated the flow of liquids from two parallel holes. We investigated how the split of the combine jets is affected by five key parameters. The surface tension γ, the radii of the holes R, the distance between the holes D, the velocity V_{out} and the dynamic viscosity μ.

Using food coloring to trace the streamlines, we found that in the single jet state the liquid flows mostly

around a central drop, with water regeneration in the drop happening only on a longer timescale. This drop was spotted to sometimes linger behind the jets after tearing of the water sheet. We hypothesized that this drop is responsible for the hysteresis. In the combined jet regime, the cohesive forces pull the jets together through the drop. Upon reaching the critical pressure the two jets split and the drop detaches from the surface. When lowering the pressure back down the drop is not there to pull the jets together anymore and no phase transition occurs.

We used the Darcy Weisbach equation to describe the friction losses, achieving a good fit for the drainage velocity measured in the laminar regime. Equipped with the connection of V_{out} and h, we focused on what occurs after the jets pass through the holes. We proposed that the transition between the single and twin jet state is caused by the battle between surface tension and inertia. With the surface tension keeping the jets together and the inertia tearing them apart. We introduce a split parameter S, with:

$$\boxed{S = \frac{V_c D}{R} \sqrt[4]{\frac{\rho}{g\gamma}}}, \tag{8.1}$$

where $S > S_{crit} = 0.23$ determines the twin jet phase. $S < S_{crit}$ determines the combined jet phase, when coming from the low pressure regime. Once the jets split they stay split even when lowering the pressure showing hysteresis, since the water drop combining them is not there anymore. S has a very weak dependance on the surface tension and density, which makes the model applicable for wide variety of liquids.

References

[1] Rayleigh, L. (1878), On The Instability Of Jets. Proceedings of the London Mathematical Society, s1-10: 4-13. https://doi.org/10.1112/plms/s1-10.1.4

[2] BUSH, J., & HASHA, A. (2004). On the collision of laminar jets: Fluid chains and fishbones. Journal of Fluid Mechanics, 511, 285-310. doi:10.1017/S002211200400967X

[3] Institute of Oceanology, Russian Academy of Sciences, Moscow 117851, Russia , "On the frontal collision of two round jets in water", Physics of Fluids 15, 3429-3433 (2003) https://doi.org/10.1063/1.1613644

[4] http://www.met.reading.ac.uk/~sws04cdw/viscosity_calc.html. The calculation is based on the parameterisation in Cheng (2008) Ind. Eng. Chem. Res. 47 3285-3288, with a number of adjustments, which are described in Volk and Kähler (2018) Experiments in Fluids 59 75.

[5] Die Jodide der Elemente aus der Stickstoffgruppe F. M. Jaeger,H. J. Doornbosch, 7 May 1912 https://doi.org/10.1002/zaac.19120750121

[6] Pierre Simon marquis de Laplace, Traité de Mécanique Céleste, volume 4, (Paris, France: Courcier, 1805), Supplément au dixième livre du Traité de Mécanique Céleste, pages 1–79

[7] rederic P. Miller, Agnes F. Vandome, McBrewster John VDM Publishing, 24 Nov 2010 Darcy-Weisbach Equation

[8] Buckingham, E. (1914). "On physically similar systems; illustrations of the use of dimensional equations". Physical Review. 4 (4): 345–376. doi:10.1103/PhysRev.4.345. hdl:10338.dmlcz/101743.

[9] Philip Day; Andreas Manz; Yonghao Zhang (28 July 2012). Microdroplet Technology: Principles and Emerging Applications in Biology and Chemistry. Springer Science & Business Media. pp. 9–. ISBN 978-1-4614-3265-4.